



Oxidation of NiAl(110)
by Wade William Brown

A thesis submitted in partial fulfillment of the requirements for the degree of Master of Science in
Physics
Montana State University
© Copyright by Wade William Brown (1990)

Abstract:

We have studied the oxidation of NiAl(110) using Auger electron spectroscopy, x-ray photoelectron spectroscopy, surface second harmonic generation measurements, and contact potential difference measurements. Oxygen forms a bond to the aluminum atoms on the (110) surface, although the oxide formed is geometrically and possibly chemically different from that formed in Al₂O₃. The adsorbed oxygen is weakly incorporated into the surface, having a sticking coefficient very much smaller than that found on any low index aluminum surface. There is little or no direct interaction between the nickel atoms in the surface region and the adsorbed oxygen. Instead, nickel serves indirectly to stabilize the surface against oxygen adsorption through the nickel-aluminum bonding of the substrate. There is no evidence that nickel is depleted in the surface region by the oxygen adsorption process. The oxide that forms under heavy exposures forms first on top of the surface and subsequently diffuses into the bulk.

OXIDATION OF NiAl(110)

by

Wade William Brown

**A thesis submitted in partial fulfillment
of the requirements for the degree**

of

Master of Science

in

Physics

**MONTANA STATE UNIVERSITY
Bozeman, Montana**

July, 1990

11378
B 8164

APPROVAL

of a thesis submitted by

Wade William Brown

This thesis has been read by each member of the thesis committee and has been found to be satisfactory regarding content, English usage, format, citations, bibliographic style, and consistency, and is ready for submission to the College of Graduate Studies.

4 Aug 90

Date

Wade W. Brown

Chairperson, Graduate Committee

Approved for the Major Department

8-14

Date

W. Brown

Head, Major Department

Approved for the College of Graduate Studies

August 15, 1990

Date

Dwight S. Parsons

Graduate Dean

STATEMENT OF PERMISSION TO USE

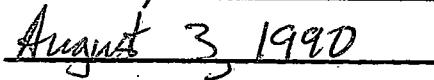
In presenting this thesis in partial fulfillment of the requirements for a master's degree at Montana State University, I agree that the Library shall make it available to borrowers under rules of the Library. Brief quotations from this thesis are allowable without special permission, provided that accurate acknowledgment of source is made.

Permission for extensive quotation from or reproduction of this thesis may be granted by my major professor, or in his/her absence, by the Dean of Libraries when, in the opinion of either, the proposed use of the material is for scholarly purposes. Any copying or use of the material in this thesis for financial gain shall not be allowed without my written permission.

Signature



Date



ACKNOWLEDGEMENTS

I would like to thank the members of my committee Dr. John L. Carlsten and Dr. Adolfo G. Eguiliz who read through this thesis carefully and offered suggestions. Dr John L. Carlsten's expertise in the area of lasers was extremely beneficial to my second harmonic generation measurements. Also, I would like to thank the staff of the CRISS facility here at Montana State University, Dr. James R. Anderson and Milton Jaehnig. They assisted my research efforts while making measurements in the CRISS facility and also assisted me when making measurements in our laboratory.

Finally, I would like to thank my advisor Dr. Wayne K. Ford, who supplied an environment that allowed me to learn about a wide range of topics in surface science. Dr. Ford also read through this thesis in its early stages and offered a great deal of help and insight.

TABLE OF CONTENTS

| | Page |
|--|------|
| APPROVAL..... | ii |
| TABLE OF CONTENTS..... | v |
| LIST OF FIGURES..... | vi |
| ABSTRACT..... | viii |
| CHAPTERS | |
| 1. INTRODUCTION..... | 1 |
| 2. EXPERIMENTAL TECHNIQUES..... | 4 |
| Sample Preparation..... | 4 |
| Auger Electron Spectroscopy..... | 9 |
| X-Ray Electron Spectroscopy..... | 15 |
| Kelvin Probe..... | 18 |
| Surface Second Harmonic Generation..... | 23 |
| 3. PREVIOUS OXIDATION STUDIES..... | 28 |
| Oxidation of Aluminum..... | 28 |
| Oxidation of Nickel..... | 35 |
| Oxidation of Nickel Aluminum..... | 39 |
| 4. EXPERIMENTAL RESULTS FOR NICKEL ALUMINUM..... | 41 |
| 5. DISCUSSION OF RESULTS..... | 54 |
| REFERENCES CITED..... | 63 |

LIST OF FIGURES

| Figure | Page |
|---|------|
| 1. Modified PHI 545 Ultra High Vacuum Chamber..... | 7 |
| 2. Sample Holder for Modified PHI 545 Chamber..... | 8 |
| 3. Auger decay process | 10 |
| 4. Auger cross section for oxygen on aluminum versus E_p/E | 13 |
| 5. Schematic of x-ray photoemission process..... | 16 |
| 6. Double charge layer..... | 19 |
| 7. Contact potential difference capacitor circuit..... | 21 |
| 8. Drawing of Kelvin probe assembly..... | 22 |
| 9. Optical setup for SHG experiment..... | 26 |
| 10. Electronics schematic for SHG experiment..... | 27 |
| 11. Three low index faces for face centered cubic lattice | 29 |
| 12. Work function change versus oxygen exposure for aluminum..... | 33 |
| 13. AES oxygen uptake for aluminum..... | 35 |
| 14. Work function change versus exposure for Ni(100) | 37 |
| 15. Oxygen uptake for Ni(111)..... | 38 |
| 16. Oxygen uptake for Ni(100)..... | 39 |
| 17. Top view of the NiAl(110) surface | 41 |
| 18. Proposed two layered rippled surface for NiAl(110)..... | 42 |
| 19. Representative Auger spectra from PHI 595 | 44 |
| 20. Normalized Auger peak heights versus O ₂ exposure for NiAl(110)..... | 45 |
| 21. Low energy aluminum and nickel Auger peaks versus exposure..... | 47 |

LIST OF FIGURES - Continued

| Figure | Page |
|--|------|
| 22. Work function change versus exposure for clean surface..... | 49 |
| 23. Work function change versus exposure for a contaminated surface..... | 50 |
| 24. Second harmonic intensity versus exposure..... | 51 |
| 25. XPS spectra for Ni 2p core levels versus oxygen exposure..... | 52 |
| 26. XPS spectra for Al 2p and Ni 3p core levels versus exposure | 53 |
| 27. Atomic concentration versus exposure..... | 60 |
| 28. Saturation atomic concentration versus oxygen exposure..... | 62 |

ABSTRACT

We have studied the oxidation of NiAl(110) using Auger electron spectroscopy, x-ray photoelectron spectroscopy, surface second harmonic generation measurements, and contact potential difference measurements. Oxygen forms a bond to the aluminum atoms on the (110) surface, although the oxide formed is geometrically and possibly chemically different from that formed in Al_2O_3 . The adsorbed oxygen is weakly incorporated into the surface, having a sticking coefficient very much smaller than that found on any low index aluminum surface. There is little or no direct interaction between the nickel atoms in the surface region and the adsorbed oxygen. Instead, nickel serves indirectly to stabilize the surface against oxygen adsorption through the nickel-aluminum bonding of the substrate. There is no evidence that nickel is depleted in the surface region by the oxygen adsorption process. The oxide that forms under heavy exposures forms first on top of the surface and subsequently diffuses into the bulk.

CHAPTER 1

INTRODUCTION

The physical properties of intermetallic alloys such as the transition metal aluminides were extensively studied first during the 1950's and 1960's and interest in these materials have continued to this day.¹ Early on many attractive properties were found: high strength at high temperatures, high corrosion resistance, and high ductility for single-crystal specimens, to name a few. In recent years with the advent of modern surface science techniques a new interest in the surface properties of the intermetallic alloys has occurred. These more microscopic tools have allowed scientists to study both bulk properties and surface phenomena with considerably greater control and reliability.

Of the intermetallic alloys, the nickel aluminides have many fundamentally interesting and technologically useful properties. The bulk properties of this family of materials stand out. For example, the yield strength of conventional alloys, such as stainless steel, decrease with increasing temperature. However, Liu and Stiegler showed for $\text{Ni}_3\text{Al}+0.2\text{B}$ the yield strength actually increases up to a temperature of about 600°C .¹ The reason for the high temperature strength of Ni_3Al is thought to be associated with the process of microalloying.¹ Microalloying is a metallurgical technique of adding small concentrations of compounds in order to enhance certain desirable properties. For the case cited above, microalloying of Ni_3Al with boron not only increases its high temperature strength but also increases its ductility by 50% over that measured for pure Ni_3Al .² This is very important to technological applications of the material because the ductility of a material determines the ease by which it can be machined.

The surface chemistry of the nickel aluminum alloys is also of technological interest because these alloys can be used as corrosion resistant materials and as heterogeneous catalysts. The application of nickel aluminum as a corrosion resistant material is technologically important because of the wide spread desire for the long term stability of products to degradation due to corrosion. The application of nickel aluminum as a heterogeneous catalyst is of technological importance because one-sixth of the value of all goods manufactured in the United States involve catalytic processes. Recent research in this area has shown that mixed-metal catalysts can provide a powerful way to control catalytic activity and selectivity.³

Notwithstanding their technological potential, the nickel aluminides offer the basic scientist a special family of materials with which to study the electronic structure of metals and metallic surfaces. There are at least three ordered stoichiometries of nickel aluminum: Ni_3Al , NiAl , and NiAl_3 . Each represents a blend of a classic simple metal with the archetypal d-band transition metal in an ordered, characterizable lattice. The relative importance of the d-band atom to the electronic, geometric, and chemical properties of the bulk alloy can be examined by comparing materials of different stoichiometries. For each stoichiometry the properties of the bands derived from the nickel 3d shell electrons will reflect both lattice and hybridization effects, the latter being due to the alloy bonding of the nearly free aluminum electrons. Heuristically speaking, the d-bands are filled as the aluminum content is increased. This is accomplished without the addition of any new d-states, as one would have, for example, in nickel copper alloys. In addition to the several bulk stoichiometries, each low index face of the crystal isolates a different relative surface composition of the aluminum and nickel atoms or presents a different aluminum-nickel intra-plane spacing. One expects that these geometric considerations will be manifest in dramatic effects in the surface electronic structure and surface chemical activity of the material.

NiAl(110) is a good choice as a model surface for experimental and theoretical studies of the surface chemical properties of the nickel aluminum alloys because it forms a stable, 50-50 stoichiometry on a microscopic scale. Our work investigates the incipient oxidation of this surface. We have sought to characterize the oxidation of NiAl(110) in the "monolayer" regime and to draw distinctions between this alloy and the oxidation properties of the more familiar aluminum and nickel surfaces. In Chapter 2 a description of the experimental methods and techniques used in the study is presented. In Chapter 3 we review what is known about the oxidation of aluminum and nickel. Our experimental results are presented in Chapter 4, and we conclude with our interpretation of those results in Chapter 5.

CHAPTER 2

EXPERIMENTAL TECHNIQUES

No one experimental probe is generally sufficient to characterize the surfaces of materials. In surface science one is forced to utilize a wide variety of techniques to address a problem. In this study of nickel aluminum x-ray photoelectron spectroscopy (XPS), Auger electron spectroscopy (AES), Kelvin probe work function analysis ($\Delta\phi$), laser second harmonic generation (SHG), and elastic low energy electron diffraction (LEED) measurements were performed using equipment in the surface science laboratories at Montana State University. In this chapter the application of these techniques and their underlying physical principles are discussed. First, the preparation of the sample is described.

Sample Preparation

The nickel aluminum single crystal was obtained from Dr. D. Zehner of Oak Ridge National Laboratory and Dr. D. Pease of the University of Connecticut. Prior to our measurements the sample orientation was checked by the method of Laue x-ray diffraction. The crystal surface orientation was determined to be within 0.5° of the (110) plane. Mechanical polishing of the (110) surface was performed by using successively finer grades of alumina polish, starting out with a $5\ \mu$ polish and finishing with a $0.05\ \mu$ polish. This sequence of polishing steps produced a surface with little light scatter when checked with a helium neon laser. A minimum amount of light scatter from the surface is important for the success of the SHG experiment. In later measurements we found that a

better optical surface could be obtained with a final polish of Syton,* a silicon based colloidal suspension. Polishing with Syton reduced further the light scatter from the surface, but changed somewhat the work function measurements. As described below, although the total change in work function with oxygen exposure was reproducible between preparation methods, the Syton polished sample reached a saturation value at a slightly lower exposure. After mechanical polishing the sample was ultrasonically cleaned in a bath of acetone, followed by a rinse of methanol.

In ultra-high vacuum the crystal was cleaned by repeated cycles of high-temperature sputtering at a sample temperature of 850°C, followed by a ten minute anneal at 850°C. No effect of cooling rate after the anneal was observed in our measurements. The sputtering was done at a primary ion beam energy of 800 eV to 1000 eV for fifteen minutes each cycle. The anneal was necessary to remove any damage done to the surface during sputtering, and, in particular, to restore the 50-50 stoichiometry of the bulk to the surface since aluminum is preferentially sputtered from nickel aluminum.⁴ The sample was considered clean when there was no detectable Auger signal from carbon or oxygen contamination. In one chamber XPS was used to establish cleanliness. In this case signal averaging was used to increase the signal to noise ratio because the cross section for x-ray ionization for these two elements is small at the available photon energies. In the other two systems surface contamination checking was done with AES. It usually took only one sputter-anneal cycle to clean the sample.

The experiments were performed using three separate ultrahigh vacuum chambers. Oxygen uptake measurements were carried out primarily in a Physical Electronics Scanning Auger Microprobe (SAM) model PHI 595. This system was equipped with a Digital Equipment PDP-11 computer that controlled a single pass cylindrical

* Remet Chemical Corp. 278 Chadwicks, N.Y. 13319

mirror analyzer (CMA) and performed data acquisition. The CMA is an energy band pass dispersive device used to measure the kinetic energy distribution of the Auger electrons. The ultra-high vacuum chamber of the 595 was pumped by an ion pump, a titanium sublimation pump, and a turbo pump. The working pressure of this system was around 5×10^{-10} Torr. The sample was held in place using the holder provided with the machine.

Other AES measurements were carried out in a modified commercial chamber, a Physical Electronics model 545, equipped as above with a single pass CMA with integral gun. A schematic of this chamber is presented in Figure 1. The AES measurements carried out in this chamber were made to monitor surface condition prior to Kelvin probe and second harmonic measurements. This chamber was also equipped with a low energy electron diffraction (LEED) apparatus and a Kelvin probe for measuring work function changes. This was the chamber in which the second harmonic generation measurements were performed. The single pass CMA was computer controlled using an ATT 6300+ microcomputer. An experimental control system was developed by adapting a general purpose experimental control program written for the ATT computer by Will Hough, an MSU undergraduate research assistant. The computer programs controlled all of the experiments performed in this chamber. This system included an ion sputter gun for sample preparation. The chamber was pumped by an ion pump, a titanium sublimation pump, and a turbo pump, which provided a working pressure of this system of around 2×10^{-10} Torr.

A third chamber, manufactured by Leybold Heraeus, was used for the XPS measurements. The vacuum was maintained with two ion pumps, two turbo pumps, and a titanium sublimation pump. The working pressure was around 1×10^{-10} Torr. Included with the chamber was a electron energy loss spectrometer, a dual anode x-ray source, and a

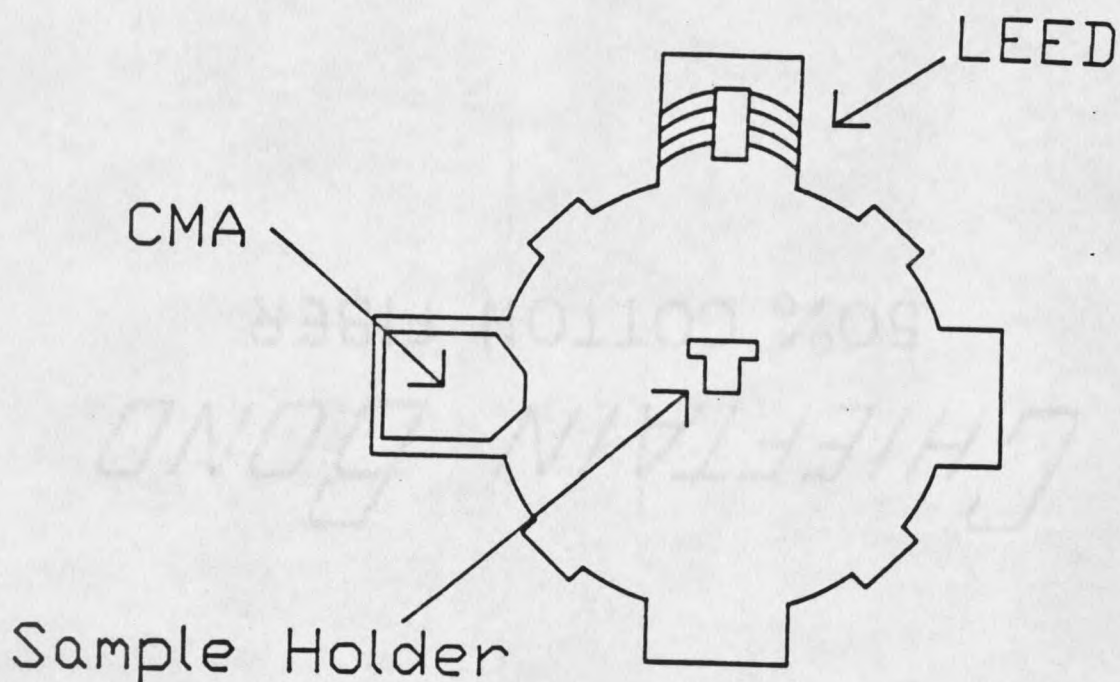


Figure 1: Modified PHI 545 Ultra High Vacuum Chamber.

hemispherical energy analyzer. Sample preparation was performed with an ion sputter gun.

A different sample holder was used for each of the three chambers used. The sample holder used in the modified 545 chamber is displayed in Figure 2. It was designed to maintain the position of sample during heating. This was important because the SHG measurements required the surface plane of the sample to remain in a constant position so as not to disturb the optical alignment of the laser and detection optics positioned outside of the vacuum vessel. The nickel aluminum crystal was machined to have a raised surface which allowed for secure mounting using a stainless steel 0.010 inch face plate. The face plate did not extend above the sample surface. Thus, shadowing effects were eliminated when the sample was cleaned using sputter ion bombardment. The sample holder was

hollowed out to form a space behind the sample. Inside this cavity was a 0.010 inch tantalum filament used as an electron source for electron bombardment heating. The sample was held at ground potential and the filament floated at a negative potential for heating. This heating arrangement gave good temperature control from 200°C to 850°C. The temperature was monitored with a chromel-alumel thermocouple. The sample was customarily heated from room temperature to 850°C in less than five minutes.

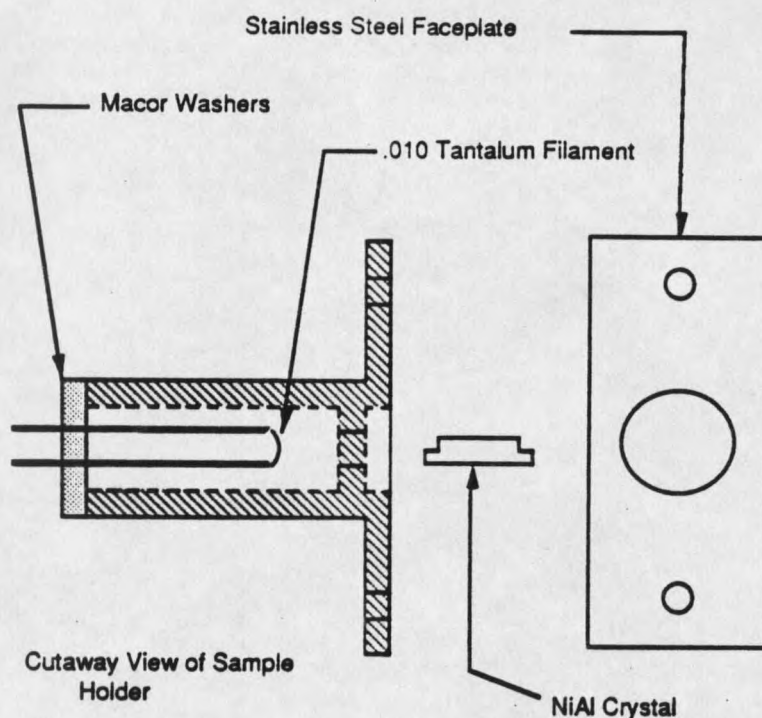


Figure 2: Sample Holder for Modified PHI 545 Chamber

In the XPS chamber the sample was mounted between two pieces of .010 inch tantalum foil. The tantalum foil pieces had holes cut out of them with the same diameter as the raised surface on the crystal. The crystal was placed between the two foil pieces, with the raised surface of the sample protruding through one of the foil pieces. Then the foil pieces were spot welded together. The foil and sample arrangement were mounted on the spectrometer manipulator over a .010 inch tantalum filament which served as an electron

source. The temperature was monitored with a platinum-platinum rhodium 10% alloy thermocouple spot welded to the sample.

Auger Electron Spectroscopy

Auger electron spectroscopy is used routinely by surface scientists to quantify the elemental composition of surfaces. A high energy beam of electrons with kinetic energies in the range of 1 keV to 10 keV is made to strike a sample surface. The penetrating beam undergoes both elastic and inelastic collisions, losing most of its energy over a depth of 10 to 20 Å.⁵ Core level electrons are ejected during collisions with the atoms of the material, leaving a trail of ions and atoms in various excited states which will decay to lower energy configurations with an emission of either a photon via x-ray fluorescence or an electron in an Auger process. The probability for x-ray emission falls off with lower atomic number and more shallow core levels. For lighter elements and shallow cores Auger emission is favored over fluorescence. An empirically derived relation giving the transition probability ω for fluorescence is given by $\omega = (1 + aZ^4)^{-1}$ where the constant 'a' has a value of 1.12×10^6 for K shell ionizations and 6.4×10^7 for L shell processes.⁶ For example, from this expression the photon transition probability is 3.2% for L shell ionizations in strontium and 3.3% for K shell ionizations in silicon. Thus, as a practical matter incident electrons with 2 keV kinetic energy will not produce appreciable x-ray fluorescence from the K, L, and M atomic shells below atomic numbers of 14 (silicon), 38 (strontium), and 76 (osmium), respectively.

A schematic view of the Auger de-excitation process is presented in Figure 3. The ejected electrons come from a core level of binding energy ϵ_1 relative to the chemical potential. An electron from an outer shell of binding energy ϵ_2 subsequently relaxes into the vacancy in the core level. The energy released in this transition is taken up by a third

electron of energy ϵ_3 which is subsequently ejected from the material. This second ejected electron is called the Auger electron. The vacuum kinetic energy of this electron E_A is given, neglecting electron correlation, by $E_A = \epsilon_1 - \epsilon_2 - \epsilon_3 - W$ where W is the work function of the material. Note that the final state of this process leaves the atom in a two-hole ionized state that can subsequently relax via Auger emission with the valence electrons.

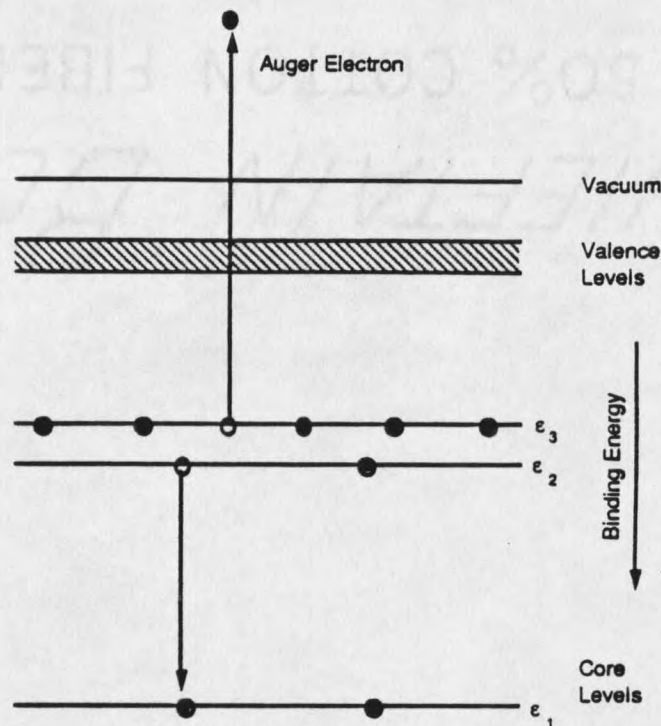


Figure 3: Auger decay process

A more complete understanding of the Auger process requires one to examine ionization cross sections and backscattering factors. Ionization cross sections give the probability of ionization for an electron atom scattering event. The backscattering factor gives a measure of the number of Auger secondary electrons that will undergo additional scattering events prior to being emitted from the sample. Ionization cross sections have been estimated previously⁷ and the total cross section $\sigma(E_p)$ was given as

$$\sigma(E_p) = \frac{2\pi e^2}{E_p E} b \ln \frac{4E_p}{B}$$

Here E_p is the energy of the incident primary electrons, E is the ionization potential, e is the charge on the electron, b is equal 0.35 for K shell electrons and 0.25 for L shell electrons, and B is a function of E_p and E . Worthington and Tomlin⁸ found B to have the following form for $E \leq E_p$:

$$B = \left\{ 1.65 + 2.35 \exp\left(1 - \frac{E_p}{E}\right) \right\} E$$

They arrived at this form of B empirically by requiring that $\sigma(E_p)$ would vanish at E_p equal to E and that the shape would be the same as had been shown experimentally.

Combining these results yields

$$\sigma(E_p) = 1.3 \times 10^{-13} \frac{b}{UE^2} \ln \left\{ \frac{4U}{1.65 + 2.35(1-U)} \right\} (cm^2)$$

where U equals E_p/E .

The result for $\sigma(E_p)$ should also be corrected to include the effect of multiply scattered and backscattered electrons. The correction term is given by

$$\sigma' = \int_E^{E_p} \sigma(E) n(E) dE$$

where $n(E)$ is the number of backscattered electrons at energy E . This correction term can be combined with $\sigma(E_p)$ to give the total corrected cross section

$$\sigma'(E_p) = \sigma(E_p) \left\{ 1 + r_m(E_p, E, \alpha) \right\}$$

where $r_m(E_p, E, \alpha)$ is the correction due to the backscattered electrons. The term $r_m(E_p, E, \alpha)$ is dependent on both the incident and ionization energies and the matrix in which the atoms are embedded, denoted by α . Reuter⁹ has empirically determined a relationship for the backscattering term. The relationship is

$$r_m(E_p, E) = 1 + 2.8\eta \left(1 - 0.9 \frac{E_p}{E} \right)$$

η is a material dependent parameter and is given in terms of atomic number by

$$\eta = -0.1254 + 0.016 Z - 0.000186 Z^2 + 8.3 \times 10^{-7} Z^3$$

In the case of aluminum ($Z = 13$) the backscattering correction term $r_m(E_p, E, \alpha)$ is equal to 1.08 for $E/E_p = 0.5$.

Figure 4 is a graph of σ and σ' versus E_p/E for the specific case of oxygen on a substrate of aluminum. The dependence of the cross section on the adatom is through the ionization energy for the adatom. By examining the figure it is seen that the σ' reaches a maximum at about E_p/E equal to about 2.6. Therefore, to maximize the probability of an oxygen Auger transition the primary energy of the beam should be 2.6 times the ionization energy of the oxygen level of interest, in this case 532 eV. The backscattering term increases the cross section at the maximum nearly a factor of two, due to the additional Auger transitions induced by the backscattered electrons.

